HHS Public Access

Author manuscript

Ocul Surf. Author manuscript; available in PMC 2024 November 09.

Published in final edited form as:

Ocul Surf. 2021 October ; 22: 135–142. doi:10.1016/j.jtos.2021.08.004.

Alterations in corneal nerves in different subtypes of dry eye disease: An *in vivo* confocal microscopy study☆

Stephanie M. Cox[a,1], **Ahmad Kheirkhah**[b,1], **Shruti Aggarwal**[b], **Farshad Abedi**[b], **Bernardo M. Cavalcanti**[b], **Andrea Cruzat**[b], **Pedram Hamrah**[a,b,*]

[a]Center for Translational Ocular Immunology and Cornea Service, Department of Ophthalmology, Tufts Medical Center, Tufts University School of Medicine, Boston, MA, USA

[b]Ocular Surface Imaging Center, Cornea & Refractive Surgery Service, Massachusetts Eye & Ear Infirmary, Department of Ophthalmology, Harvard Medical School, Boston, MA, USA

Abstract

Purpose: To evaluate corneal subbasal nerve alterations in evaporative and aqueous-deficient dry eye disease (DED) as compared to controls.

Methods: In this retrospective, cross-sectional, controlled study, eyes with a tear break-up time of less than 10 s were classified as DED. Those with an anesthetized Schirmer's strip of less than 5 mm were classified as aqueous-deficient DED. Three representative *in vivo* confocal microscopy images were graded for each subject for total, main, and branch nerve density and numbers.

Results: Compared to 42 healthy subjects (42 eyes), the 70 patients with DED (139 eyes) showed lower total (18,579.0 ± 687.7 μm/mm^2 vs. 21,014.7 ± 706.5, p = 0.026) and main (7,718.9 ± 273.9 vs. 9,561.4 ± 369.8, p < 0.001) nerve density, as well as lower total (15.5 ± 0.7/frame vs. 20.5 ± 1.3, p = 0.001), main (3.0 ± 0.1 vs. 3.8 ± 0.2, p = 0.001) and branch (12.5 ± 0.7 vs. 16.5 ± 1.2, p = 0.004) nerve numbers. Compared to the evaporative DED group, the aqueous-deficient DED group showed reduced total nerve density (19,969.9 ± 830.7 vs. 15,942.2 ± 1,135.7, p = 0.006), branch nerve density (11,964.9 ± 749.8 vs. 8,765.9 ± 798.5, p = 0.006) total nerves number (16.9 ± 0.8/frame vs. 13.0 ± 1.2, p = 0.002), and branch nerve number (13.8 ± 0.8 vs. 10.2 ± 1.1, p = 0.002).

Conclusions: Patients with DED demonstrate compromised corneal subbasal nerves, which is more pronounced in aqueous-deficient DED. This suggests a role for neurosensory abnormalities in the pathophysiology of DED.

☆**Meeting presentation:** This work was presented, in part, at the American Academy of Ophthalmology Annual Meeting, October 2014.

*Corresponding author. Cornea Service, New England Eye Center/Tufts Medical Center, Department of Ophthalmology, Tufts University School of Medicine, Boston, MA, USA. pedram.hamrah@tufts.edu, p_hamrah@yahoo.com (P. Hamrah).
[1]These authors contributed equally to this work.

Disclosure/conflicts of interest

Financial support was provided by the Imaging Fellowship Heidelberg Engineering, Tufts Medical Center Institutional Support, Allergan, Inc, United States., Falk Medical Research Trust, and Allergan Inc. PH and BMC are patent inventors. Other authors have no potential conflicts of interest.

Keywords

Corneal nerves; Dry eye disease; In vivo confocal microscopy

1. Introduction

Dry eye disease (DED) is one of the most common disorders of the eye [1]. The 2017 Dry Eye Workshop II (DEWS II) defined DED as "a multifactorial disease of the ocular surface characterized by a loss of homeostasis of the tear film, and accompanied by ocular symptoms, in which tear film instability and hyperosmolarity, ocular surface inflammation and damage, and neurosensory abnormalities play etiological roles" [2]. The neurosensory aspect of DED includes corneal sensory innervation, which is then transmitted and processed within the central nervous system causing tear production via parasympathetic innervation. The cornea is the most densely innervated tissue in the human body For the purposes of this study, it is important to note that a nerve plexus called the subbasal nerve plexus exists at the interface between Bowman's layer and the basal epithelial cells, and its anatomical integrity can be assessed using *in vivo* confocal microscopy (IVCM) [3–6].

Previous studies using IVCM have found that the corneal nerves are affected in patients with a variety of conditions [3–6], including diabetes 7–9, fibromyalgia [10], multiple sclerosis [11,12], rheumatoid arthritis [13], HIV [14], orthokeratology lens wear [15,16], myopia [17], corneal infections 18–24, corneal dystrophies [25–28], DED [29–35], and neuropathic corneal pain (NCP) [36–38]. One study investigated non-Sjögren's DED vs. Sjögren's syndrome DED and demonstrated that subbasal nerve density was reduced in non-Sjögren's DED as compared to control subjects, and was reduced by a larger amount in Sjögren's syndrome DED [31]. Two additional studies investigated DED unrelated to ocular graft-versus-host disease vs. DED caused by ocular graft-versus-host disease, but neither showed a significant difference in subbasal nerve density between these groups [33, 34]. However, no published literature has reported on corneal nerve differences between evaporative DED and aqueous-deficient DED, the most common types of DED.

Evaporative DED refers to the process by which the tear film evaporates from the ocular surface due to conditions such as meibomian gland dysfunction, while aqueous-deficient DED refers to patients with a reduced tear volume [39]. Reduced tear volume suggests reduced tear production, which, as referenced previously, is in part mediated by corneal nerves. Therefore, an investigation into differences in corneal nerves between these groups would strengthen the theorized relationship between reduced corneal nerve density and reduced tear production in aqueous-deficient DED. This finding of reduced corneal nerve density would guide researchers and clinicians toward treatments aimed at increasing corneal nerve density within aqueous-deficient DED patients. Thus, we hypothesized that both types of DED will have a reduced subbasal corneal nerve density compared to control subjects and that aqueous-deficient DED patients will have a greater reduction compared to evaporative DED patients, given the involvement of the lacrimal gland. This study aims to assess if total, main, and/or branch nerves vary in evaporative and aqueous-deficient DED.

2. Material and methods

2.1. Study design and patients

In this cross-sectional, retrospective, controlled study, the study group consisted of subjects with a clinical diagnosis of DED, and the control group consisted of a sample of subjects from a reference control database [19,40]. The study group included all patients from the Cornea Service, Massachusetts Eye & Ear Infirmary, Harvard Medical School, Boston, Massachusetts seen by one of the authors (P.H.) between 2009 and 2012, who met the inclusion/exclusion criteria outlined below and had an IVCM dataset available for analysis. The reference control database was prospectively enrolled and was designed to provide IVCM data for comparison in our IVCM studies. While IVCM is performed during routine clinical assessment of patients with corneal infections and ocular surface disease (and thus allowing for retrospective analysis), it is not performed on normal patients during their routine clinical assessments. Therefore, the reference control database used in this study was designed to provide IVCM data for comparison to data collected during routine clinical assessment of diseased samples. Subjects included in this database reported no symptoms of ocular discomfort, had no corneal or conjunctival staining, fluorescein tear break-up time (TBUT) >10 s, and had an anesthetized Schirmer's wetting test of >15mm. To avoid bias of subject selection from this database, the entire database was initially included in the control group and then the youngest control subjects were excluded one by one until the control and DED groups did not differ significantly in age or sex. The protocol of the study was approved by the Institutional Review Board/Ethics Committee, complied with the Health Insurance Portability and Accountability Act (HIPAA) and adhered to the tenets of the Declaration of Helsinki.

The exclusion criteria in both the study group and the reference control groups included use of topical anti-glaucoma or anti-inflammatory medications, active ocular allergy, a history of contact lens wear or infectious keratitis in the past three months, and a history of ocular surgery in the past six months. DED for the study group was diagnosed clinically with the presence of typical DED symptoms for more than 6 months, such as dryness, irritation, discomfort, foreign body sensation, burning, stinging, light sensitivity, and intermittent blurriness, as well as a TBUT < 10 s. Subjects within the study group were classified as evaporative DED if they had an anesthetized Schirmer's wetting test of greater than 5 mm. Subjects were classified as aqueous-deficient, if they had an anesthetized Schirmer's wetting test of less than or equal to 5 mm. Of note, one subject from the DED group did not have both eyes included in the analysis because one eye did not meet the inclusion criteria for the evaporative DED or aqueous-deficient DED groups. When acquiring the study group data, the protocol allowed for collection of data from both eyes. In the protocol for collection of data for the control database, only one eye's data was collected per subject.

2.2. In vivo confocal imaging

IVCM image acquisition for all DED and control subjects was completed using the Heidelberg Retina Tomograph 3 with Rostock Cornea Module (Heidelberg Engineering GmbH, Heidelberg, Germany) equipped with a ×63 objective lens, a numerical aperture of 0.9 (Olympus, Tokyo, Japan), and a 670-nm red wavelength diode laser source, as

previously described [19]. Digital images were recorded with the sequence mode at a rate of 30 frames per second, including 100 images per sequence. There was a separation of 1 μm between adjacent images, and a lateral resolution of 1 μm/pixel. A total of six to eight sequence scans of non-overlapping areas were recorded from the full thickness of the central cornea, with 3–4 sequence scans focusing on the subbasal layer, resulting in 300–400 images of the subbasal layer alone per patient. The subbasal plexus is seen in subepithelial area, immediately at or posterior to the basal epithelial layer and anterior to the Bowman's layer, typically at a depth of 50–80 μm.

2.3. Image analysis

Representative non-overlapping images were selected by a masked observer (A.K.) based on sharpness of focus, lack of motion, and good contrast. Two masked graders (A.K, F.A.) analyzed three representative images from the 300–400 subbasal images for each eye, performed using the semi-automated tracing program NeuronJ (http://www.imagescience.org/meijering/software/neuronj/) [41], a plug-in for ImageJ software (developed by Wayne Rasband, National Institutes of Health, Bethesda, MD; available at http://rsb.info.nih.gov/ij/http://rsb.info.nih.gov/ij/) as previously described [19]. The following metrics were assessed: (1) *Total nerve density* was assessed by measuring the total length of the nerve fibers in micrometers per frame (160,000 μm^2) (Fig. 1); (2) Main nerve trunks were defined as the total *number of main nerve trunks* in one image after analyzing the images anterior and posterior to the analyzed image to confirm that these did not branch from other nerves; (3) *Nerve branching* was defined as the total number of nerve branches in one image; (4) The number of *total nerves* measured was defined as the number of all nerves, including main nerve trunks and branches in one image. The data were expressed as density ($\mu m/mm^2$) ± SEM. For each IVCM parameter, an intra-grader average of the three images from each subject was calculated. If the difference between the two intra-grader averages was less than 10%, an inter-grader average for each IVCM parameter values was calculated and used for analysis. In case of any discrepancy, the images were analyzed by a third grader.

2.4. Statistical analysis

IBM SPSS version 21 (IBM Corp., Armonk, NY) was used for all statistical analyses. Kolmogorov-Smirnov was used to determine normality. Independent *t*-test and chi-square tests were used to analyze for differences in age and sex, respectively, between the groups. In the study group, data for each eye was collected. Therefore, for these subjects, percent difference between the eyes was determined. To determine if the eyes should be treated individually for analysis purposes, Wilcoxon signed-rank test was used to determine if the percent differences were significantly different from a hypothesized zero difference. Two sets of generalized estimating equation analyses were performed to test for differences in IVCM parameters between groups. Both included age as a covariate due to previous literature that suggested that age could impact corneal nerves [30,35], and subject was included as a random variable to account for correlation between eyes. The first set tested for differences between the control and DED groups for each of the IVCM parameters, and the second set tested for differences between the control, evaporative DED, and aqueous-deficient DED groups. In the second, differences between groups were identified via post-

hoc pairwise comparison testing within the generalized estimating equation analysis module, which uses the marginal means from the model, with Bonferroni correction.

3. Results

3.1. Demographics

This study included 139 eyes of 70 patients with DED (42 females and 28 males) and 42 eyes of 42 normal control subjects (26 females and 16 males). There was no difference in the sex distribution between the groups (p = 0.842). The average age (±standard error) of the DED and control subjects was 54.2 ± 2.0 years and 49.7 ± 1.6 years, respectively (p = 0.077). Table 1 provides the demographics for the control and DED groups. Within the DED group, 91 (65.5%) eyes were classified as having evaporative DED and 48 (34.5%) were classified as having aqueous-deficient DED. Demographics for the evaporative and aqueous-deficient DED groups were not provided since within the same subject, one eye could classify as evaporative and the other eye as aqueous-deficient.

3.2. Clinical signs

The DED group had an average (±standard error) TBUT of 4.1 ±0.2 s (n = 139 eyes) and an average Schirmer's strip result of 9.8 ± 0.6 mm (n = 139 eyes). These values for the evaporative DED group were 4.6 ± 0.2 s (n = 91 eyes) and 13.5 ± 0.6 mm (n = 91 eyes). For the aqueous-deficient DED group, the average TBUT was 3.2 ± 0.3 s (n = 48 eyes), and the average Schirmer's strip results were 2.9 ± 0.2 mm (n = 48 eyes).

3.3. Comparisons between eyes

The average (±standard error) percent difference between eyes for total, main, and branch nerve densities were 29.5 ± 5.0%, 35.6 ± 5.1%, and 39.0 ± 5.4%, respectively. The average (±standard error) percent difference between eyes for number of total, main, and branch nerves were 35.2 ± 5.1%, 36.5 ± 5.1%, and 40.0 ± 5.4%, respectively. Because these percent differences were significantly different from zero (all p < 0.001), the eyes were treated individually within the analysis.

3.4. Corneal nerve alterations by IVCM

The summary for morphological nerve parameters for eyes with DED and normal control groups are reported in Table 2. Representative IVCM images from each DED subgroups and controls are shown in Fig. 2. Table 2 and Figs. 3–6 provide descriptive statistics of the IVCM parameters for each group.

The average (±standard error) total, main, and branch nerve densities for all the DED patients were 18,579.0 ± 687.7 μm/mm^2, 7718.9 ± 273.9, and 10,860.2 ± 576.0, respectively These values for control group were 21,038.1 ± 720.5, 9,581.4 ± 394.9, and 11,296.8 ± 557.9, respectively. Differences between the control (Fig. 2A) and DED groups (Fig. 2B and C) were identified by the first models, which showed a significant effect of group on the models for total nerve density ($\chi^2_1 = 4.979$, $p = 0.026$) and main nerve density ($\chi^2_1 = 12.153$, $p < 0.001$) (Fig. 3). However, there was no significant effect of group identified in the branch nerve density model ($\chi^2_1 = 0.293$, $p = 0.588$). The average number of total, main, and

branch nerves for the DED group were 15.5 ± 0.7/frame (96.9 ± 4.4/mm^2), 3.0 ± 0.1 (18.8 ± 0.6), and 12.5 ± 0.7 (78.1 ± 4.4), respectively. These same values for the control group were 20.5 ± 1.3/frame (125.0 ± 7.5/mm^2), 3.8 ± 0.2 (23.8 ± 1.3), and 16.5 ± 1.2 (103.1 ± 7.5), respectively. There was a significant difference in total (χ_1^2 = 11.446, p = 0.001), main (χ_1^2 = 11.637, p = 0.001), and branch (χ_1^2 = 8.317, p = 0.004) nerve numbers between these groups (Fig. 4). The results of the generalized estimating equation model comparing the control and DED group showed that age had no significant effect on any of the confocal nerve findings (all p > 0.05).

The average total, main, and branch nerve densities for the evaporative DED group were 19,969.9 ± 830.7 μm/mm^2, 8,005.0 ± 313.1, and 11,964.9 ± 749.8, respectively. These values for the aqueous-deficient DED group were 15,942.2 ± 1,135.7 μm/mm^2, 7,176.3 ± 522.2, and 8,765.9 ± 798.5. In the second set of models, which included these subgroups of DED and the control group, a significant effect of group was identified for total nerve density (χ_2^2 = 11.592, p = 0.003), main nerve density (χ_2^2 = 12.915, p = 0.002), and branch nerve density (χ_2^2 = 8.325, p = 0.016). Pairwise comparisons were needed to identify between group differences in these models because more than two groups were used in the model. Fig. 5 shows these pairwise comparisons between the groups based on marginal means. The control group exhibited a significantly higher main nerve density compared to the evaporative DED group. All density parameter values were increased in the control group compared to the aqueous-deficient DED. There was also an increased total nerve density and branch nerve density in the evaporative DED group compared to the aqueous-deficient DED group. The average total, main, and branch nerve counts for the evaporative DED group were 16.9 ± 0.8/frame (105.6 ± 5.0/mm^2), 3.1 ± 0.1 (19.4 ± 0.6), and 13.8 ± 0.8 (86.3 ± 5.0), respectively. These same values for the aqueous-deficient DED group were 13.0 ±1.2 (81.3 ±7.5), 2.8 ±0.2 (15.6 ± 1.3), and 10.2 ± 1.1 (63.8 ± 6.9), respectively. The models showed a significant effect of group on models for total (χ_2^2 = 21.798, p < 0.001), main (χ_2^2 = 21.476, p = 0.002), and branch (χ_2^2 = 19.493, p < 0.001) nerve numbers, and Fig. 6 shows the pairwise comparisons between the groups based on marginal means. The control group exhibited significantly more total nerves and main nerves per image compared to the evaporative DED group. All nerve number parameter values were increased in the control group compared to the aqueous-deficient DED. The number of total nerves and branch nerves per image were increased in evaporative DED compared to aqueous-deficient DED. The results of the generalized estimating equation model that included control, evaporative DED, and aqueous-deficient DED also showed that age did not have a significant effect on any of the confocal nerve findings (all p > 0.05).

3.5. Post-hoc power

The total nerve density data was used for the calculation of the power for this study. Because the aim of the study was to identify differences between evaporative DED and aqueous-deficient DED, the means and standard errors of these groups as listed in Table 2 were used for the power analysis. Using this data, the power of this study was 81.0%.

4. Discussion

Herein, we report a statistically significant reduction in total, main, and branch nerve numbers and nerve density in a large cohort of DED patients compared to controls. Moreover, we demonstrate that this reduction is significantly more pronounced in aqueous-deficient DED as compared to the evaporative DED. Total nerve density reported by this study falls between total nerve density values reported previously 19, 29–31,33,36–38,42], which range from 15,956 (SD = 2,431) to 26, 422.8 (SD = 4,491.0) μm/mm^2. The total nerve density reported by this study for the DED group was slightly higher than values reported previously 29,30,33,34,37,42,43, which range from 9,426 (SD = 2,640) [29] to 18,300 (SD = 5,100) μm/mm^2 [34]. The value reported for the evaporative DED group is higher than this range, and the aqueous deficient DED group is within this range. Some studies used an automated software for quantification of nerves; however, these studies reported lower total nerve density, total nerve count, and total branch nerve count values compared to values reported using the semi-automated technique used here [44–46]. In addition, the evaporative DED group showed values that were similar to that identified in previous literature, which used criteria similar to that outlined in this study [47].

Previous IVCM studies have shown nerve alterations in DED, these reports have been inconsistent [29–31,35,42,48]. While some studies have report reduced nerve density patients with DED compared to normal controls [29–31,35,42,37], none have compared nerve alterations between the most common types of DED, namely evaporative and aqueous-deficient DED. One study reported a higher nerve density in a DED group compared to controls, but this difference was not statistically significant [49]. However, it appears that the control group had characteristics consistent with DED, such as reduced Schirmer's strip scores, which could explain the inconsistency with other studies in the literature. A second study reported that a larger number of nerves were present in Sjögren's syndrome aqueous-deficient DED patients compared to controls and non-Sjögren's aqueous deficient DED subjects [50]. However, this study utilized a white-light confocal microscope device, which has lower resolution as compared to the laser IVCM [5,51]. However, no study to date has provided a direct comparison between the two major types of DED, evaporative and aqueous-deficient DED.

Compared to other ocular conditions, the loss of subbasal corneal nerve plexus seen with DED is less pronounced. Patients with toxic keratopathy [52], ocular graft-versus-host-disease [33], and limbal stem cell deficiency [53] shows greater loss in nerve density, as do patients with Fuchs' endothelial corneal dystrophy and bullous keratopathy [54]. In addition, eyes with herpetic infections 20,38,55 have greater loss of corneal nerves than DED patients or their subgroups. However, interestingly, the main nerve density of both DED subgroups and the combined DED group is similar to the unaffected eyes of unilateral herpes zoster ophthalmicus patients, and the number of branches and total number of nerves is greater in our DED sample compared to the unaffected eyes of herpes zoster ophthalmicus patients [20]. Aqueous-deficient DED group has a similar total nerve density compared to the unaffected eyes of herpes zoster ophthalmicus patients [20] and eyes with keratoconus [56].

Studies have also used IVCM to assess the presence of inflammatory cells [19,20,31,46,57–62]. A negative correlation between inflammation and nerve density has been identified in many of these studies [19, 20,31,57]. Evidence has also shown that patients with Fuchs' endothelial corneal dystrophy [54], infectious keratitis [19,20], DED [31,61], and autoimmune disease [31] have a reduction in nerve density and an increase in inflammatory cell density compared with controls. The results of this study along with a previous study, which reported higher levels of inflammation in aqueous-deficient DED compared to evaporative DED using the same diagnostic criteria as that outlined in this study [63], only further supports the association between inflammation and corneal innervation. This association has led many to investigate the relationship between immune cells and nerves, which is now commonly termed neuro-immune crosstalk [64]. Neuro-immune crosstalk typically begins with an increased presence of inflammation. This increased presence of inflammation could be caused by trauma, autoimmune conditions, or disease/pathology. However, it is also possible that stimulation of the corneal sensory nerves, which release pro-inflammatory mediators could cause the increase in the density of inflammatory cells [65–68]. It is important to note that the presence of increased inflammation is established as part of the pathogenesis of dry eye disease [69]. Cytokines produced by immune cells are recognized by receptors on nerves, which may result in nerve degradation [70].

It is unclear if aqueous-deficiency may result in nerve fiber loss or if the nerve fiber loss causes aqueous-deficiency. The lacrimal functional unit, which transmits corneal sensations to the lacrimal glands, begins with the afferent sensory corneal nerves of the cornea, which travel from the cornea to the trigeminal nucleus of the brain stem [71]. From the trigeminal nucleus, ascending neurons project to the thalamus and superior salivatory-lacrimal nucleus [72,73]. The thalamic path then continues to the primary somatosensory cortex [74], and the superior salivatory-lacrimal nucleus pathway continues to the pteryopalantine ganglion and lacrimal gland [75]. It is through the superior salivatory-lacrimal nucleus pathway that stimulation of the corneal nerves can cause lacrimation [76]. Therefore, degeneration of the corneal nerves caused by any inflammatory event or trauma could disrupt the superior salivatory-lacrimal nucleus pathway and cause decreased tear production. However, it is also possible that reduced aqueous production itself may result in increased inflammation and thereby nerve loss.

Loss of corneal nerves has several clinical implications. We have previously demonstrated in a randomized double-masked controlled clinical trial that DED patients with near-normal nerve density respond significantly better in both symptoms and corneal fluorescein staining to artificial tear and anti-inflammatory treatment compared to DED patients that presented with significantly diminished corneal nerves; however, only the steroid treatment improved nerve density [77]. Given that IVCM is not available for routine clinical use in practice, our current study would suggest that DED patients without aqueous-deficiency may respond symptomatically better to treatments than those with aqueous deficiency and that it may be beneficial to provide steroid treatment to those with aqueous-deficiency in order to improve their nerve status. Furthermore, the association between inflammation and nerve density is important when considering the development of neuropathic corneal pain in patients [37]. It was previously outlined that the aqueous-deficient eyes in this study had a lower nerve density and based on our prior study also a higher dendritiform cell density compared to the

evaporative DED group [63]. This presence of nerve damage and concurrent inflammation can theoretically result in peripheral nerve sensitization and the development of neuropathic pain [78]. Thus, both the increased inflammation and nerve damage observed in the aqueous-deficient DED group within the cornea suggests that these patients may be at a higher risk for neuropathic corneal pain.

Despite demonstrating the differential impact of DED subtypes on corneal nerve density and neurosensory abnormalities, our study has several limitations. The retrospective nature of the study did not allow us to have a full data set on patient symptom questionnaires for the diagnosis of DED, although all patients did have symptoms of DED for more than 6 months and the same experienced clinician assessed all patients. The diagnosis of DED was also limited to utilization of TBUT and Schirmer's test due to the retrospective nature of this study. Future prospective studies will allow for more extensive parameters. In addition, while evaporative and aqueous deficiency were defined subtypes of DED, the DEWS II criteria present this now as a continuum with severity of both components that is more difficult to separate. Since, given the inclusion criteria, the TBUT was less than 10 s in all patients DED, we used the Schirmer's test as a measure for tear secretion, to categorize the patients into these two subtypes of evaporative and aqueous-deficient DED. Therefore, the aqueous-deficient DED patients have both low Schirmer's test values and low TBUT. Eyes with pure aqueous tear deficiency and normal TBUT are not included in the current study, as most all patients have some evaporative component as highlighted by the DEWS II report. Another limitation to this study is that there was no assessment of the Meibomian glands beyond TBUT; therefore, the contribution of corneal nerve changes on gland dysfunction or vice versa cannot be assessed further. Moreover, only the central cornea was assessed for nerve alterations, and thus the results cannot be generalized to the peripheral cornea. Nevertheless, the current study provides, for the first time, a detailed quantitative assessment of subbasal nerve alterations for IVCM images in patients with evaporative and aqueous-deficient forms of DED, which may aid in the improved assessment of neurosensory abnormalities in DED, further elucidating the pathogenesis of this complex disease. Additional future studies to further expand our knowledge of DED could include an investigation of how severity of DED is associated with inflammation and nerve changes and how treatment could impact these IVCM parameters. Furthermore, the presence or absence of autoimmune conditions, and in particular autoimmune-mediated (dysimmune) small fiber neuropathy on corneal nerve alterations need to be further investigated.

5. Conclusions

In conclusion, patients with predominantly evaporative or aqueous-deficient DED demonstrate differential decrease in corneal subbasal nerves, suggesting the presence of neurosensory abnormalities in DED. These changes can be detected and quantified objectively by corneal IVCM, allowing its use for clinical practice and clinical trials. Clinicians may also find it helpful to focus treatment on increasing corneal nerve density of DED patients, especially those with the aqueous-deficient type.

Abbreviations:

DED	Dry eye disease
IVCM	in vivo confocal microscopy
TBUT	tear break up time

References

[1]. Stapleton F, Alves M, Bunya VY, et al. TFOS DEWS II epidemiology report. Ocul Surf 2017;15(3):334–65. [PubMed: 28736337]

[2]. Craig JP, Nichols KK, Akpek EK, et al. TFOS DEWS II definition and classification report. Ocul Surf 2017;15(3):276–83. [PubMed: 28736335]

[3]. Kokot J, Wylegala A, Wowra B, Wojcik L, Dobrowolski D, Wylegala E. Corneal confocal sub-basal nerve plexus evaluation: a review. Acta Ophthalmol 2018;96(3):232–42. [PubMed: 28741902]

[4]. Yang AY, Chow J, Liu J. Corneal innervation and sensation: the eye and beyond. Yale J Biol Med 2018;91(1):13–21. [PubMed: 29599653]

[5]. Cruzat A, Qazi Y, Hamrah P. In vivo confocal microscopy of corneal nerves in Health and disease. Ocul Surf 2017;15(1):15–47. [PubMed: 27771327]

[6]. Dua HS, Said DG, Messmer EM, et al. Neurotrophic keratopathy. Prog Retin Eye Res 2018;66:107–31. [PubMed: 29698813]

[7]. Xiong Q, Lu B, Ye HY, et al. Corneal confocal microscopy as a non-invasive test to assess diabetic peripheral neuropathy. Diabetes Res Clin Pract 2018;136:85–92. [PubMed: 29221815]

[8]. Markoulli M, You J, Kim J, et al. Corneal nerve morphology and tear film substance P in diabetes. Optometry and vision science. official publication of the American Academy of Optometry; 2017. p. 726–31. 94(7).

[9]. Tummanapalli SS, Issar T, Yan A, Kwai N, Poynten AM, Krishnan AV, et al. Corneal nerve fiber loss in diabetes with chronic kidney disease. Ocul Surf 2020;18(1):178–85. 10.1016/j.jtos.2019.11.010. [PubMed: 31770601]

[10]. Erkan Turan K, Kocabeyoglu S, Unal-Cevik I, Bezci F, Akinci A, Irkec M. Ocular surface alterations in the context of corneal in vivo confocal microscopic characteristics in patients with fibromyalgia. Cornea 2018;37(2):205–10. [PubMed: 29135602]

[11]. Mikolajczak J, Zimmermann H, Kheirkhah A, et al. Patients with multiple sclerosis demonstrate reduced subbasal corneal nerve fibre density. Mult Scler 2017;23(14):1847–53. [PubMed: 27811337]

[12]. Bitirgen G, Akpinar Z, Malik RA, Ozkagnici A. Use of corneal confocal microscopy to detect corneal nerve loss and increased dendritic cells in patients with multiple sclerosis. JAMA Ophthalmol 2017;135(7):777–82. [PubMed: 28570722]

[13]. Villani E, Galimberti D, Viola F, Mapelli C, Del Papa N, Ratiglia R. Corneal involvement in rheumatoid arthritis: an in vivo confocal study. Invest Ophthalmol Visual Sci 2008;49(2):560–4. [PubMed: 18234999]

[14]. Kemp HI, Petropoulos IN, Rice ASC, et al. Use of corneal confocal microscopy to evaluate small nerve fibers in patients with human immunodeficiency virus. JAMA Ophthalmol 2017;135(7):795–800. [PubMed: 28594979]

[15]. Lum E, Golebiowski B, Swarbrick HA. Reduced corneal sensitivity and sub-basal nerve density in long-term orthokeratology lens wear. Eye Contact Lens 2017;43(4):218–24. [PubMed: 27541967]

[16]. Nombela-Palomo M, Felipe-Marquez G, Teus MA, Hernandez-Verdejo JL, Nieto-Bona A. Long-term impacts of orthokeratology treatment on sub-basal nerve plexus and corneal sensitivity responses and their reversibility. Eye Contact Lens 2018;44(2):91–6. [PubMed: 28410280]

[17]. Harrison WW, Putnam NM, Shukis C, et al. The corneal nerve density in the subbasal plexus decreases with increasing myopia: a pilot study. Ophthalmic Physiol Opt 2017;37(4):482–8. [PubMed: 28656670]

[18]. Marcos-Fernandez MA, Tabernero SS, Herreras JM, Galarreta DJ. Impact of herpetic stromal immune keratitis in corneal biomechanics and innervation. Graefe's archive for clinical and experimental ophthalmology = Albrecht von Graefes Archiv fur klinische und experimentelle Ophthalmologie 2018;256(1):155–61.

[19]. Cruzat A, Witkin D, Baniasadi N, et al. Inflammation and the nervous system: the connection in the cornea in patients with infectious keratitis. Invest Ophthalmol Vis Sci 2011;52(8):5136–43. [PubMed: 21460259]

[20]. Cavalcanti BM, Cruzat A, Sahin A, Pavan-Langston D, Samayoa E, Hamrah P. In vivo confocal microscopy detects bilateral changes of corneal immune cells and nerves in unilateral herpes zoster ophthalmicus. Ocul Surf 2018;16(1):101–11. [PubMed: 28923503]

[21]. Hamrah P, Cruzat A, Dastjerdi MH, et al. Unilateral herpes zoster ophthalmicus results in bilateral corneal nerve alteration: an in vivo confocal microscopy study. Ophthalmology 2013;120(1):40–7. [PubMed: 22999636]

[22]. Muller RT, Pourmirzaie R, Pavan-Langston D, et al. In vivo confocal microscopy demonstrates bilateral loss of endothelial cells in unilateral herpes simplex keratitis. Invest Ophthalmol Visual Sci 2015;56(8):4899–906. [PubMed: 26225629]

[23]. Hamrah P, Sahin A, Dastjerdi MH, et al. In Vivo confocal microscopic changes of the corneal epithelium and stroma in patients with herpes zoster ophthalmicus. Am J Ophthalmol 2015;159(6). 1036–1044.e1031. [PubMed: 25748579]

[24]. Hamrah P, Cruzat A, Dastjerdi MH, et al. Corneal sensation and subbasal nerve alterations in patients with herpes simplex keratitis: an in vivo confocal microscopy study. Ophthalmology 2010;117(10):1930–6. [PubMed: 20810171]

[25]. Bucher F, Adler W, Lehmann HC, et al. Corneal nerve alterations in different stages of Fuchs' endothelial corneal dystrophy: an in vivo confocal microscopy study. Graefe's archive for clinical and experimental ophthalmology = Albrecht von Graefes Archiv fur klinische und experimentelle Ophthalmologie 2014;252(7): 1119–26.

[26]. Germundsson J, Lagali N. Pathologically reduced subbasal nerve density in epithelial basement membrane dystrophy is unaltered by phototherapeutic keratectomy treatment. Invest Ophthalmol Visual Sci 2014;55(3):1835–41. [PubMed: 24569577]

[27]. Patel DV, Grupcheva CN, McGhee CN. Imaging the microstructural abnormalities of meesmann corneal dystrophy by in vivo confocal microscopy. Cornea 2005;24(6):669–73. [PubMed: 16015084]

[28]. Rosenberg ME, Tervo TM, Gallar J, et al. Corneal morphology and sensitivity in lattice dystrophy type II (familial amyloidosis, Finnish type). Invest Ophthalmol Visual Sci 2001;42(3):634–41. [PubMed: 11222521]

[29]. Labbe A, Alalwani H, Van Went C, Brasnu E, Georgescu D, Baudouin C. The relationship between subbasal nerve morphology and corneal sensation in ocular surface disease. Invest Ophthalmol Visual Sci 2012;53(8):4926–31. [PubMed: 22695962]

[30]. Levy O, Labbe A, Borderie V, et al. Increased corneal sub-basal nerve density in patients with Sjogren syndrome treated with topical cyclosporine A. Clin Exp Ophthalmol 2017;45(5):455–63. [PubMed: 27957797]

[31]. Tepelus TC, Chiu GB, Huang J, et al. Correlation between corneal innervation and inflammation evaluated with confocal microscopy and symptomatology in patients with dry eye syndromes: a preliminary study. Graefe's archive for clinical and experimental ophthalmology = Albrecht von Graefes Archiv fur klinische und experimentelle Ophthalmologie. 2017;255(9):1771–8.

[32]. Tuisku IS, Konttinen YT, Konttinen LM, Tervo TM. Alterations in corneal sensitivity and nerve morphology in patients with primary Sjögren's syndrome. Exp Eye Res 2008;86(6):879–85. [PubMed: 18436208]

[33]. Tepelus TC, Chiu GB, Maram J, et al. Corneal features in ocular graft-versus-host disease by in vivo confocal microscopy. Graefe's archive for clinical and experimental

ophthalmology = Albrecht von Graefes. Archiv fur klinische und experimentelle Ophthalmologie 2017;255(12):2389–97.

[34]. Kheirkhah A, Qazi Y, Arnoldner MA, Suri K, Dana R. In vivo confocal microscopy in dry eye disease associated with chronic graft-versus-host disease. Invest Ophthalmol Visual Sci 2016;57(11):4686–91. [PubMed: 27607414]

[35]. Labbe A, Liang Q, Wang Z, et al. Corneal nerve structure and function in patients with non-sjogren dry eye: clinical correlations. Invest Ophthalmol Visual Sci 2013; 54(8):5144–50. [PubMed: 23833066]

[36]. Aggarwal S, Colon C, Kheirkhah A, Hamrah P. Efficacy of autologous serum tears for treatment of neuropathic corneal pain. Ocul Surf 2019;17(3):532–9. 10.1016/j.jtos.2019.01.009. [PubMed: 30685437]

[37]. Moein HR, Akhlaq A, Dieckmann G, Abbouda A, Pondelis N, Salem Z, et al. Visualization of microneuromas by using in vivo confocal microscopy: An objective biomarker for the diagnosis of neuropathic corneal pain? Ocul Surf 2020;18(4):651–6. 10.1016/j.jtos.2020.07.004. [PubMed: 32663518]

[38]. Bayraktutar BN, Ozmen MC, Muzaaya N, Dieckmann G, Koseoglu ND, Müller RT, et al. Comparison of clinical characteristics of post-refractive surgery-related and post-herpetic neuropathic corneal pain. Ocul Surf. 2020;18(4):641–50. 10.1016/j.jtos.2020.07.006. [PubMed: 32707336]

[39]. Wolffsohn JS, Arita R, Chalmers R, et al. TFOS DEWS II diagnostic methodology report. Ocul Surf 2017;15(3):539–74. [PubMed: 28736342]

[40]. Qazi Y, Kheirkhah A, Blackie C, et al. Clinically relevant immune-cellular metrics of inflammation in meibomian gland dysfunction. Invest Ophthalmol Vis Sci 2018;59(15):6111–23. [PubMed: 30592499]

[41]. Meijering E, Jacob M, Sarria JC, Steiner P, Hirling H, Unser M. Design and validation of a tool for neurite tracing and analysis in fluorescence microscopy images. Cytometry Part A : the journal of the International Society for Analytical Cytology 2004;58(2):167–76. [PubMed: 15057970]

[42]. Kheirkhah A, Satitpitakul V, Hamrah P, Dana R. Patients with dry eye disease and low subbasal nerve density are at high risk for accelerated corneal endothelial cell loss. Cornea 2017;36(2):196–201. [PubMed: 28060067]

[43]. John T, Tighe S, Sheha H, et al. Corneal nerve regeneration after self-retained cryopreserved amniotic membrane in dry eye disease. J Ophthalmol 2017;2017:6404918. [PubMed: 28894606]

[44]. Giannaccare G, Pellegrini M, Bernabei F, et al. In vivo confocal microscopy automated morphometric analysis of corneal subbasal nerve plexus in patients with dry eye treated with different sources of homologous serum eye drops. Cornea 2019;38(11):1412–7. [PubMed: 31090592]

[45]. Giannaccare G, Pellegrini M, Sebastiani S, Moscardelli F, Versura P, Campos EC. In vivo confocal microscopy morphometric analysis of corneal subbasal nerve plexus in dry eye disease using newly developed fully automated system. Graefe's archive for clinical and experimental ophthalmology = Albrecht von Graefes Archiv fur klinische und experimentelle Ophthalmologie 2019;257(3):583–9.

[46]. Chinnery HR, Naranjo Golborne C, Downie LE. Omega-3 supplementation is neuroprotective to corneal nerves in dry eye disease: a pilot study. Ophthalmic Physiol Opt 2017;37(4):473–81. [PubMed: 28295445]

[47]. Villani E, Magnani F, Viola F, et al. In vivo confocal evaluation of the ocular surface morpho-functional unit in dry eye. Optometry and vision science. official publication of the American Academy of Optometry; 2013. p. 576–86. 90(6).

[48]. Alhatem A, Cavalcanti B, Hamrah P. In vivo confocal microscopy in dry eye disease and related conditions. Semin Ophthalmol 2012;27(5–6):138–48. [PubMed: 23163268]

[49]. Semeraro F, Forbice E, Nascimbeni G, et al. Effect of autologous serum eye drops in patients with sjogren syndrome-related dry eye: clinical and in vivo confocal microscopy evaluation of the ocular surface. In vivo (athens, Greece) 2016;30(6):931–8. [PubMed: 27815483]

[50]. Zhang M, Chen J, Luo L, Xiao Q, Sun M, Liu Z. Altered corneal nerves in aqueous tear deficiency viewed by in vivo confocal microscopy. Cornea 2005;24(7):818–24. [PubMed: 16160498]

[51]. Erie JC, McLaren JW, Patel SV. Confocal microscopy in ophthalmology. Am J Ophthalmol 2009;148(5):639–46. [PubMed: 19674730]

[52]. Chen Y, Le Q, Hong J, Gong L, Xu J. In vivo confocal microscopy of toxic keratopathy. Eye 2017;31(1):140–7. [PubMed: 27740620]

[53]. Caro-Magdaleno M, Alfaro-Juarez A, Montero-Iruzubieta J, et al. In vivo confocal microscopy indicates an inverse relationship between the sub-basal corneal plexus and the conjunctivalisation in patients with limbal stem cell deficiency. Br J Ophthalmol 2019;103(3):327–31. [PubMed: 29777047]

[54]. Aggarwal S, Cavalcanti BM, Regali L, et al. In vivo confocal microscopy shows alterations in nerve density and dendritiform cell density in Fuchs' endothelial corneal dystrophy. Am J Ophthalmol 2018;196:136–44. [PubMed: 30194928]

[55]. Moein HR, Kheirkhah A, Muller RT, Cruzat AC, Pavan-Langston D, Hamrah P. Corneal nerve regeneration after herpes simplex keratitis: a longitudinal in vivo confocal microscopy study. Ocul Surf 2018;16(2):218–25. [PubMed: 29305292]

[56]. Pahuja NK, Shetty R, Nuijts RM, et al. An in vivo confocal microscopic study of corneal nerve morphology in unilateral keratoconus. BioMed Res Int 2016;2016:5067853. [PubMed: 26904679]

[57]. Colorado LH, Markoulli M, Edwards K. The relationship between corneal dendritic cells, corneal nerve morphology and tear inflammatory mediators and neuropeptides in healthy individuals. Curr Eye Res 2019;44(8):840–8. [PubMed: 30909745]

[58]. He J, Ogawa Y, Mukai S, et al. In vivo confocal microscopy evaluation of ocular surface with graft-versus-host disease-related dry eye disease. Sci Rep 2017;7(1):10720. [PubMed: 28878217]

[59]. Lin H, Li W, Dong N, et al. Changes in corneal epithelial layer inflammatory cells in aqueous tear-deficient dry eye. Invest Ophthalmol Visual Sci 2010;51(1):122–8. [PubMed: 19628746]

[60]. Machetta F, Fea AM, Actis AG, de Sanctis U, Dalmasso P, Grignolo FM. In vivo confocal microscopic evaluation of corneal langerhans cells in dry eye patients. Open Ophthalmol J 2014;8:51–9. [PubMed: 25317216]

[61]. Nicolle P, Liang H, Reboussin E, et al. Proinflammatory markers, chemokines, and enkephalin in patients suffering from dry eye disease. Int J Mol Sci 2018;19(4).

[62]. Shetty R, Sethu S, Deshmukh R, et al. Corneal dendritic cell density is associated with subbasal nerve plexus features, ocular surface disease index, and serum vitamin D in evaporative dry eye disease. BioMed Res Int 2016;2016:4369750. [PubMed: 26904676]

[63]. Kheirkhah A, Rahimi Darabad R, Cruzat A, et al. Corneal epithelial immune dendritic cell alterations in subtypes of dry eye disease: a pilot in vivo confocal microscopic study. Invest Ophthalmol Visual Sci 2015;56(12):7179–85. [PubMed: 26540656]

[64]. Hamrah P, Seyed-Razavi Y, Yamaguchi T. Translational immunoimaging and neuroimaging demonstrate corneal neuroimmune crosstalk. Cornea 2016;35(Suppl 1):S20–s24. [PubMed: 27631352]

[65]. Lopez MJ, Seyed-Razavi Y, Jamali A, Harris DL, Hamrah P. The chemokine receptor CXCR4 mediates recruitment of CD11c+ conventional dendritic cells into the inflamed murine cornea. Invest Ophthalmol Visual Sci 2018;59(13):5671–81. [PubMed: 30489627]

[66]. Fink DM, Connor AL, Kelley PM, Steele MM, Hollingsworth MA, Tempero RM. Nerve growth factor regulates neurolymphatic remodeling during corneal inflammation and resolution. PloS One 2014;9(11):e112737. [PubMed: 25383879]

[67]. Namavari A, Chaudhary S, Ozturk O, et al. Semaphorin 7a links nerve regeneration and inflammation in the cornea. Invest Ophthalmol Visual Sci 2012;53(8):4575–85. [PubMed: 22700709]

[68]. Tran MT, Ritchie MH, Lausch RN, Oakes JE. Calcitonin gene-related peptide induces IL-8 synthesis in human corneal epithelial cells. J Immunol 2000;164(8):4307–12. [PubMed: 10754330]

[69]. Belmonte C, Nichols JJ, Cox SM, et al. TFOS DEWS II pain and sensation report. Ocul Surf 2017;15(3):404–37. [PubMed: 28736339]

[70]. Sternberg EM. Neural regulation of innate immunity: a coordinated nonspecific host response to pathogens. Nat Rev Immunol 2006;6(4):318–28. [PubMed: 16557263]

[71]. Marfurt CF, Echtenkamp SF. Central projections and trigeminal ganglion location of corneal afferent neurons in the monkey, Macaca fascicularis. J Comp Neurol 1988;272(3):370–82. [PubMed: 2843578]

[72]. Hirata H, Hu JW, Bereiter DA. Responses of medullary dorsal horn neurons to corneal stimulation by CO(2) pulses in the rat. J Neurophysiol 1999;82(5):2092–107. [PubMed: 10561390]

[73]. Hirata H, Takeshita S, Hu JW, Bereiter DA. Cornea-responsive medullary dorsal horn neurons: modulation by local opioids and projections to thalamus and brain stem. J Neurophysiol 2000;84(2):1050–61. [PubMed: 10938327]

[74]. Moulton EA, Becerra L, Rosenthal P, Borsook D. An approach to localizing corneal pain representation in human primary somatosensory cortex. PloS One 2012;7(9):e44643. [PubMed: 22973463]

[75]. Toth IE, Boldogkoi Z, Medveczky I, Palkovits M. Lacrimal preganglionic neurons form a subdivision of the superior salivatory nucleus of rat: transneuronal labelling by pseudorabies virus. J Auton Nerv Syst 1999;77(1):45–54. [PubMed: 10494749]

[76]. Situ P, Simpson TL. Interaction of corneal nociceptive stimulation and lacrimal secretion. Invest Ophthalmol Visual Sci 2010;51(11):5640–5. [PubMed: 20554608]

[77]. Kheirkhah A, Dohlman TH, Amparo F, et al. Effects of corneal nerve density on the response to treatment in dry eye disease. Ophthalmology 2015;122(4):662–8. [PubMed: 25542519]

[78]. Dieckmann G, Goyal S, Hamrah P. Neuropathic corneal pain: approaches for management. Ophthalmology 2017;124(11s):S34–s47. [PubMed: 29055360]

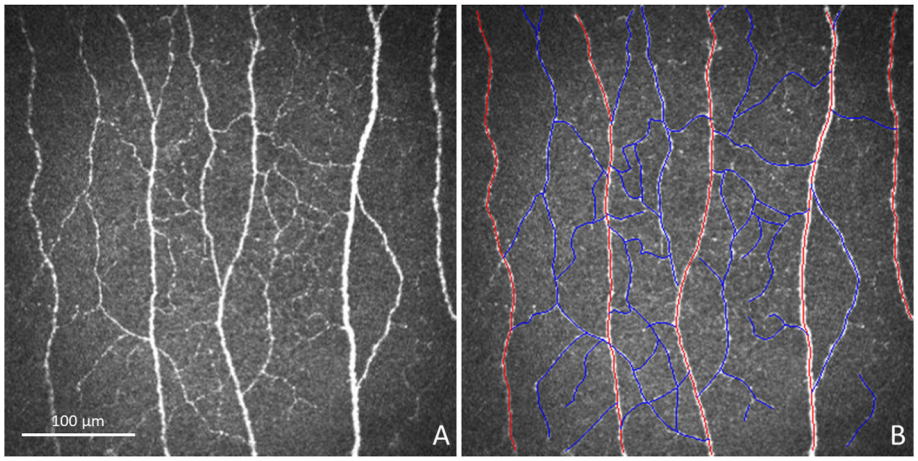

Fig. 1. Confocal Image Analysis Methodology.

Illustration of confocal image analysis methodology can be observed in the *in vivo* confocal image provided to each grader (A) and in the same image with the nerves traced (B). Red tracings highlight main nerves, and blue tracings highlight branch nerves.

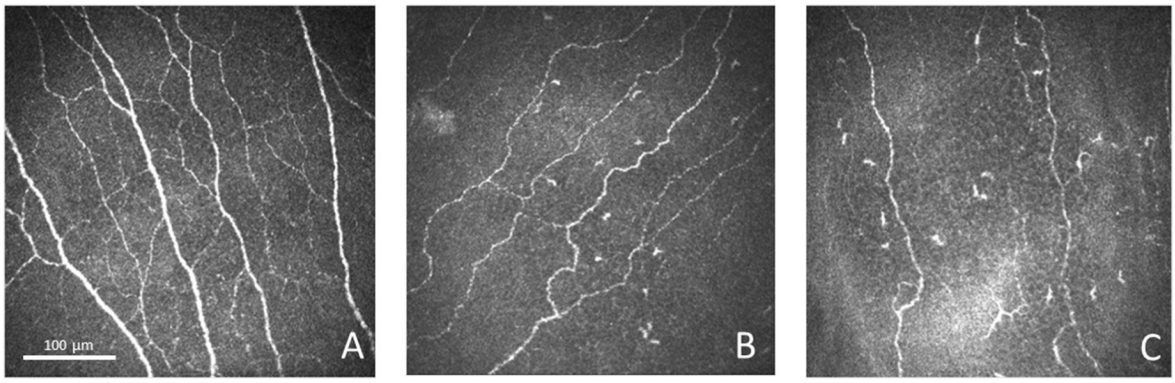

Fig. 2. IVCM Images for Each Group.

Representative IVCM images obtained at the level of the corneal subbasal nerve plexus for the control group (A), evaporative DED group (B), and aqueous-deficient DED group (C).

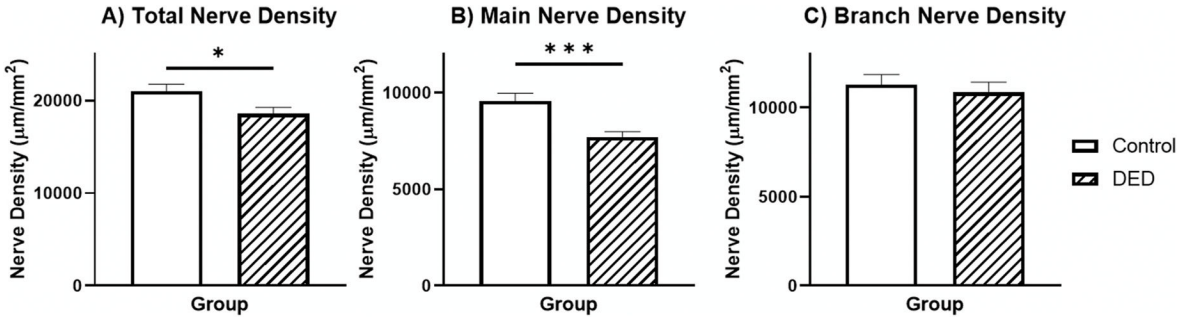

Fig. 3. Comparison of Nerve Density between Controls and DED.

Bar graph showing average for the total (A), main (B), and branch (C) nerve density for each group. Error bars represent standard error of the mean. Horizontal bars indicate significant differences between groups (* indicates $p < 0.05$, ** indicates $p < 0.005$, *** indicates $p < 0.001$).

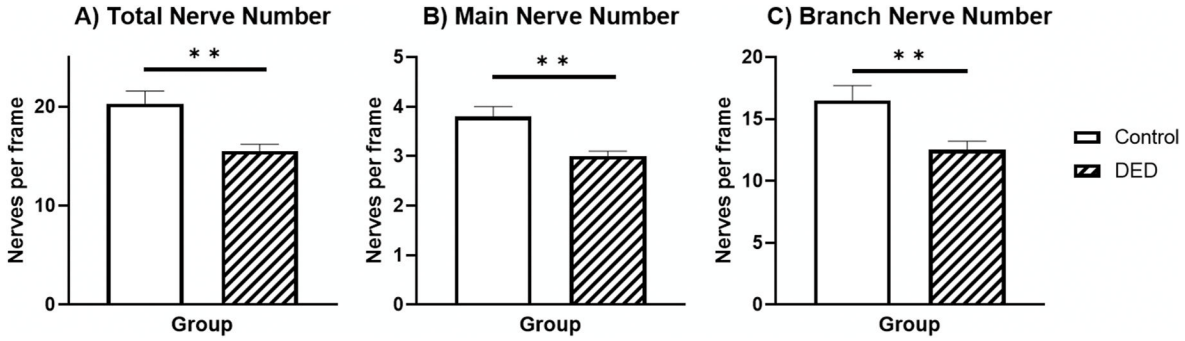

Fig. 4. Comparison of Nerve Numbers between Controls and DED.

Bar graph showing average for the total (A), main (B), and branch (C) nerve number per frame for each group. Error bars represent standard error of the mean. Horizontal bars indicate significant differences between groups (* indicates $p < 0.05$, ** indicates $p < 0.005$, *** indicates $p < 0.001$).

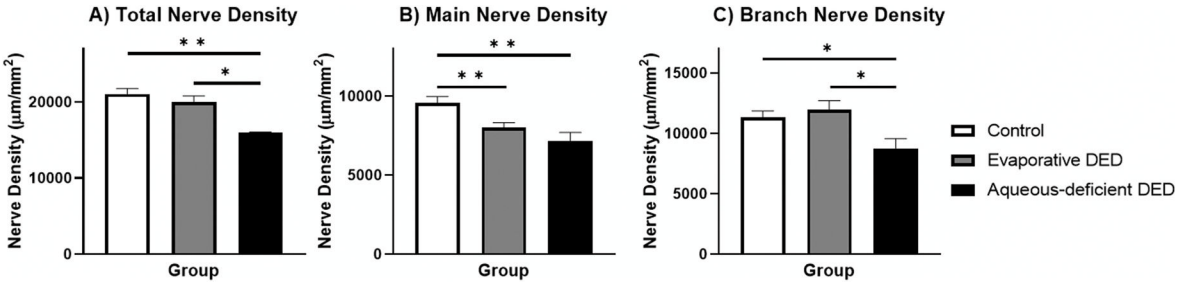

Fig. 5. Comparison of Nerve Density between Controls, Evaporative DED, and Aqueous-Deficient DED.

Bar graph showing average for the total (A), main (B), and branch (C) nerve density for each group. Error bars represent standard error of the mean. Horizontal bars indicate significant differences between groups based on post-hoc pairwise comparisons after use of generalized estimating equation analysis and Bonferroni correction (* indicates $p < 0.016$, ** indicates $p < 0.005$, *** indicates $p < 0.001$).

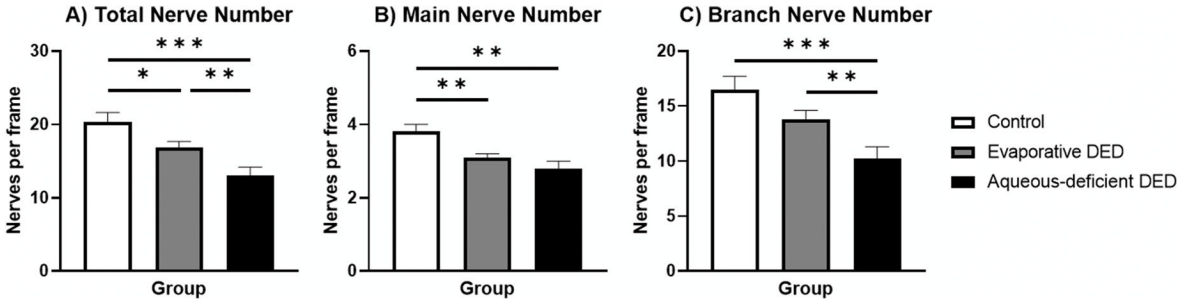

Fig. 6. Comparison of Nerve Numbers between Controls, Evaporative DED, and Aqueous-Deficient DED.

Bar graph showing average for the total (A), main (B), and branch (C) nerve number per frame for each group. Error bars represent standard error of the mean. Horizontal bars indicate significant differences between groups based on post-hoc pairwise comparisons after use of generalized estimating equation analysis and Bonferroni correction (* indicates $p < 0.016$, ** indicates $p < 0.005$, *** indicates $p < 0.001$).

Table 1

Descriptive statistics for the control and DED groups.

	Control	All DED	p-value
Number of subjects	45	70	-
Number of eyes	45	139	-
Age (mean ± standard deviation	49.7 ± 1.6 years	54.2 ± 2.0 years	0.077
Sex distribution (female/male)	26/16	42/28	0.842

Table 2

In vivo confocal microscopy parameters for corneal nerves in controls and dry eye disease patients.

	Control	All DED	Evaporative DED	Aqueous-deficient DED
n (eyes)	42	139	91	48
Total nerve density (μm/mm^2)	21,038.1 ± 720.5	18,579.0 ± 687.7[a]	19,969.9 ± 830.7	15,942.2 ± 1,135.7[a,b]
Main nerve density (μm/mm^2)	9,581.4 ± 394.9	7,718.9 ± 273.9[a]	8,005.0 ± 313.1[a]	7,176.3 ± 522.2[a]
Branch nerve density (μm/mm^2)	11,296.8 ± 557.9	10,860.2 ± 576.0	11,964.9 ± 749.8	8,765.9 ± 798.5[a,b]
Total nerves per frame (n/mm^2)	20.5 ± 1.3 (125.0 ± 7.5)	15.5 ± 0.7[a] (96.9 ± 4.4)	16.9 ± 0.8[a] (105.6 ± 5.0)	13.0 ± 1.2[a,b] (81.3 ± 7.5)
Main nerves per frame (n/mm^2)	3.8 ± 0.2 (23.8 ± 1.3)	3.0 ± 0.1[a] (18.8 ± 0.6)	3.1 ± 0.1[a] (19.4 ± 0.6)	2.8 ± 0.2[a] (15.6 ± 1.3)
Branch nerves per frame (n/mm^2)	16.5 ± 1.2 (103.1 ± 7.5)	12.5 ± 0.7[a] (78.1 ± 4.4)	13.8 ± 0.8 (86.3 ± 5.0)	10.2 ± 1.1[a,b] (63.8 ± 6.9)

All parameters are presented as mean ± standard error.

[a] Indicates significant difference compared to control group.

[b] Indicates significant difference between evaporative DED and aqueous-deficient DED groups.